

A Cryoprotectant-Gel Composite Designed to Preserve Articular Cartilage during Frozen Osteoarticular Autograft Reconstruction for Malignant Bone Tumors: An Animal-Based Study

Chao-Ming Chen^{1,2,3,4} , Yi-Chun Chen^{1,2} , Jir-You Wang^{1,2,5},
 Cheng-Fong Chen^{1,2,4}, Kuang-Yu Chao^{1,2}, Po-Kuei Wu^{1,2,4} ,
 and Wei-Ming Chen^{1,2,4}

Abstract

Objective. We designed a highly adhesive cryoprotectant-gel composite (CGC), based on regular liquid-form cryoprotectant base (CB), aiming to protect cartilage tissue during frozen osteoarticular autograft reconstruction for high-grade sarcoma around the joint. This study aimed to evaluate its effectiveness in rat and porcine distal femur models. **Design.** Fresh articular cartilage samples harvested from distal rat and porcine femurs were divided into 4 test groups: untreated control group, liquid nitrogen (LN) freezing group, LN freezing group pretreated with CB (CB group), and LN freezing group pretreated with CGC (CGC group). Microscopic and macroscopic evaluation of cartilage condition, TUNEL (terminal deoxynucleotidyl transferase dUTP nick end labeling) assay, and apoptotic protein analysis of chondrocytes were performed to confirm our results. **Results.** In the rat model, CGC could prevent articular cartilage from roughness and preserve more proteoglycans when compared with the LN freezing and CB groups. Western blot analysis showed CGC could prevent cartilage from LN-induced apoptosis supported by caspase-3/8 apoptotic signaling cascade. Macroscopically, we observed CGC could reduce both articular clefting and loss of articular luminance after freezing in the porcine model. In both models, CGC could reduce articular chondrocytes from degeneration. Fewer TUNEL-positive apoptotic and more viable chondrocytes in cartilage tissue were observed in the CGC group in our animal models. **Conclusion.** Our study proved that CGC could effectively prevent cartilage surface and chondrocytes from cryoinjury after LN freezing. Freezing articular cartilage surrounded with high concentration of CGC can be a better alternative to preserve articular cartilage during limb salvage surgery for malignant bone tumor.

Keywords

cartilage cryoinjury, cartilage cryopreservation, vitrification, bone sarcoma, osteoarticular reconstruction

Introduction

Primary bone sarcomas often develop in skeletally immature patients, located mainly in the metaphyseal region, and often involve critical joints. Expandable endoprosthesis reconstruction reduces the risk of leg length discrepancy. It preserves the function of the joint, but there are still many complications, such as implant structure failure, aseptic loosening, and disturbance of the adjacent physis.¹⁻³ Therefore, some surgeons would choose osteoarticular bone grafting to manage bone defects after tumor excision to restore bone stock and preserve the affected joint's function.^{3,4} For patients with intact bony integrity, a recycled osteoarticular autograft can be used: the excised, tumor-contained bone graft would

¹Department of Orthopaedic & Traumatology, Taipei Veterans General Hospital, Taipei City, Taiwan

²Therapeutical and Research Center of Musculoskeletal Tumor, Taipei Veterans General Hospital, Taipei City, Taiwan

³Institute of Clinical Medicine, School of Medicine, National Yang Ming Chiao Tung University, Hsinchu, Taiwan

⁴Department of Orthopaedic, School of Medicine, National Yang Ming Chiao Tung University, Hsinchu, Taiwan

⁵Institute of Traditional Medicine, School of Medicine, National Yang Ming Chiao Tung University, Hsinchu, Taiwan

Corresponding Author:

Po-Kuei Wu, Department of Orthopaedic & Traumatology, Taipei Veterans General Hospital, 201, Section 2, Shih-Pai Road, Taipei City 112, Taiwan.

Email: drwuvgh@gmail.com



be subjected to tumor eradication procedure (extracorporeal irradiation [ECIR], pasteurization, or liquid nitrogen [LN] freezing) and then transplanted back to patients.^{3,5,6} For patients with disrupted bony integrity, osteoarticular allograft would be an alternative.

It is crucial to preserve the integrity of live chondrocytes and cartilage for either osteoarticular autograft or allograft or allograft. When the tumor-containing osteoarticular autografts are treated with either ECIR or pasteurization to kill tumor cells, no effective methods are reported to preserve the innocent articular cartilage. On the other hand, water is the most abundant component in the matrix and contributes up to 80% of its net weight in the superficial and intermediate layers of the cartilage.^{7,8} During LN freezing to kill tumor cells or for freeze-storage of allograft in a tissue bank, water within the articular matrix would become ice. The resultant osmotic dehydration would damage both chondrocytes and the resultant osmotic dehydration proteoglycan networks.⁹⁻¹² Therefore, some authors apply the concept of vitrification in tissue preservation to preserve cartilage and chondrocytes from injury during rapid freezing.^{10,13}

Various formulas of cryoprotectants have been developed to protect articular cartilage. VS55 (a combination of 3.1 M dimethyl sulfoxide [DMSO], 2.2 M propylene glycol, 3.1 M formamide) is one of the most commonly used to restore cartilage tissue in a tissue bank. However, the protocol is complicated and takes more than 90 minutes for vitrification.^{14,15} Hayashi *et al.*¹⁶ and Onari *et al.*¹⁷ also reported that the ethylene glycol (EG)-based method protects cartilage during cryotherapy for bone tumors. Recently, Shardt *et al.*¹⁸ proposed an engineered protocol to preserve cartilage for osteochondral allograft and shortened loading time to 7 hours. However, when trying to use either of these methods to protect the cartilage, we have to immerse cartilage along with some part of the epiphyseal bone and the tumor tissue, if the tumor also invades epiphysis, into the cryoprotectant solution. In this way, selective cryoprotection of the articular cartilage only cannot be achieved. Therefore, we developed a new cryoprotectant-gel composite (CGC) formula that is very sticky and will persistently adhere to the joint surface to protect the cartilage, even during LN freezing. This study aimed to use animal models to simulate cryotherapy and verify the efficacy of the CGC formula to prevent cartilage from cryoinjury during LN freezing.

Materials and Methods

Preparation of CGC and Characterization

To enhance the viscosity and stickiness of the cryoprotectant during LN freezing, we produced a novel gel composite of cryoprotectant. First, liquid-form cryoprotectant base (CB), a mixture of EG (63 g, 10 M), DMSO (10 g, 1.2 M), sucrose (17 g, 0.5 M), and 27 g normal saline, was heated to 70 °C. Second, sodium polyacrylate (molecular weight:

120,000) was added to CB in a 1:10 ratio (sodium polyacrylate:CB) and then cooled down to gain CGC. Because of CGC's highly adhesive and hydrophilic properties, the cartilage surface could be well covered with CGC during the entire course of LN freezing (Fig. 1A-C). The CGC is a noncrystalline solid and will not form crystallized ice during freezing (Fig. 1D and E). To understand the permeation of the cryoprotectants into the hyaline cartilage, we used thermogravimetric analysis (TGA) to understand the change of H₂O content within the vitrified hyaline cartilage. CGC was applied on joint surface for 24 hours, 60 minutes, and 15 minutes, respectively, for analysis. In addition to a negative control without any treatment, we also immersed the whole osteoarticular graft in CB solution (rather than selectively vitrify cartilage only) for 24 hours as a positive control. After treatment, the whole layer of the hyaline cartilage samples was harvested right away and subjected to TGA analysis (SDT Q600®; TA Instruments, New Castle, DE) within the range of 27 °C to 240 °C with the rate of 3 °C/min. The analysis was carried out in a nitrogen atmosphere (200 ml/min) to guarantee an inert environment and avoid the experimental error caused by the production of water molecules in the cartilage during the oxygenated heating process. Data plotted as residual weight in percentage versus temperature were obtained and subjected to polynomial regression on SigmaPlot to obtain TGA curves of different groups.

Experimental Design and Surgical Procedure

This 2-part study used a rat model (6-month-old male *Rattus norvegicus*) to understand how CGC worked to protect cartilage.¹⁹ After that, we used a distal porcine femur model (5- to 7-month-old male Lanyu Landrace porcine, from the National Laboratory Animal Center) to simulate tumor cryoablation, as in clinical practice. The mean articular thickness of the porcine model was around 2.23 mm (range, 1.9-2.7 mm), similar to the cartilage thickness of human lower limbs (range, 1.65-2.98 mm).^{18,20} All animals received analgesia before they were sacrificed to harvest bone specimens. Swine were then subjected to electronacrosis by applying 200 V of high-frequency alternating current (about 1,500 Hz) to the head, which would not be felt and resulted in an electric shock without muscle contraction. The distal femur and its articular cartilage were harvested immediately, followed by different experiments in a separate room. Distal femurs (including whole layer of cartilage, epiphyseal and metaphyseal bone tissue) harvested from rats and porcine ($n = 6$) were all immersed in an insulated barrel filled with two-thirds full of LN for 20 minutes (Fig. 1). During the immersion process, we would continuously monitor the liquid nitrogen level. If the level became lower than the bone tissue, we would immediately fill it up. After freezing, the specimens would be wrapped in 2 sterilized towels in a separate stainless steel tray at room temperature for 15

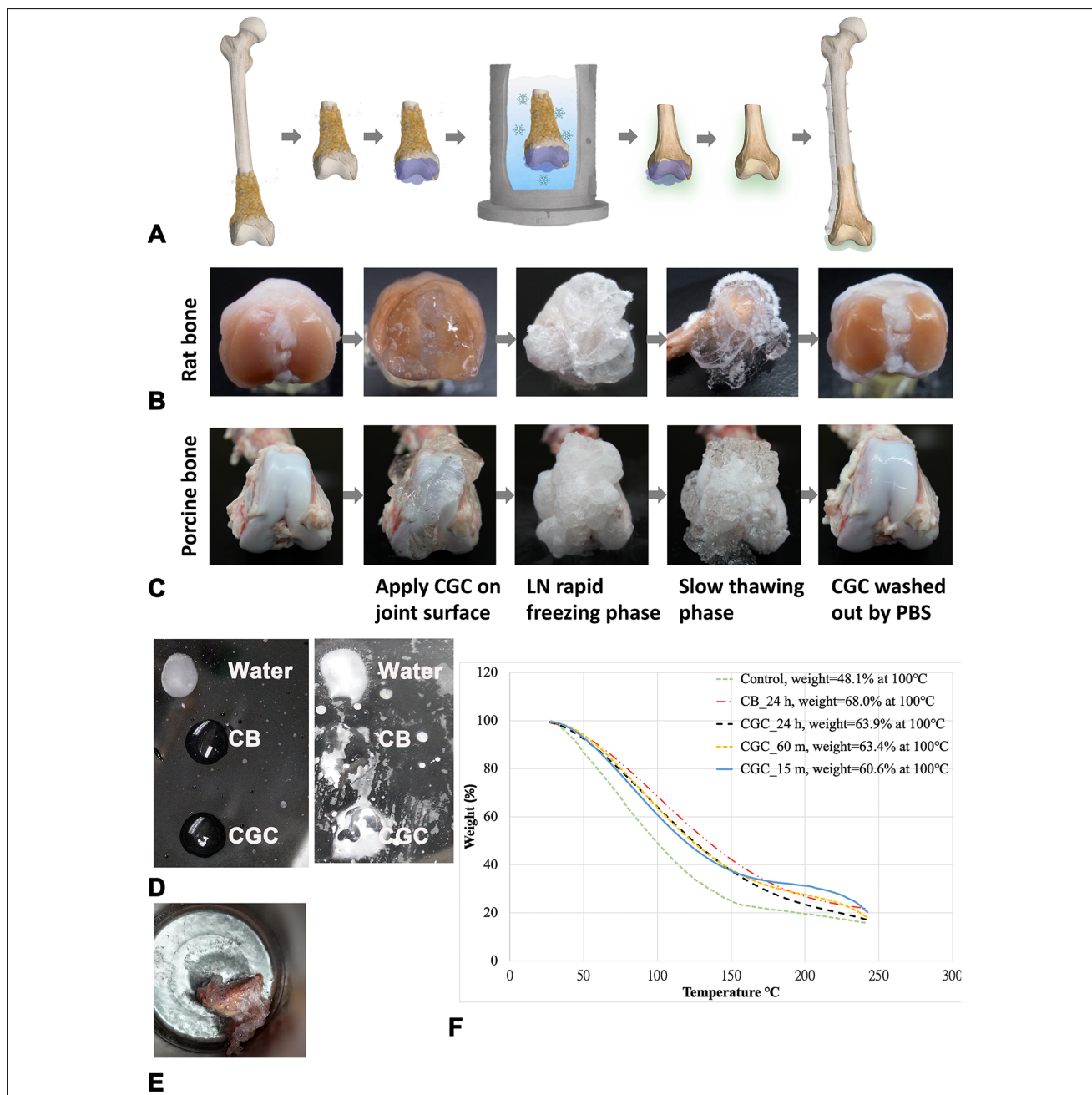


Figure 1. (A) The schematic diagram of an application of CGC in recycled osteoarticular autograft reconstruction for malignant bone tumor. After wide excision of the tumor, the CGC will be applied on the joint surface to vitrify articular cartilage. The bone with the tumor will be immersed into LN to kill tumor cells. After slow thawing at room temperature, the CGC will be washed away, and the osteoarticular autograft will be fixed to the host bone. Ligament reconstruction will also be done. (B-C) The flow diagram of applying CGC on the joint surface of the distal femur of rat (B) and porcine (C). The CGC was applied on the joint surface for 5 minutes in the rat model and for 15 minutes in the porcine model, followed by direct LN soaking and freezing for 20 minutes to vitrify cartilage tissue. After cryotherapy, the bone graft was kept at room temperature for slow thawing (15 minutes). The CGC was then washed away with PBS. (D) LN freezing experiments on droplets of water, CB, and CGC on a Petri dish in a closed LN freezing system. Both CB and CGC were in the form of a noncrystalline solid and will not form crystallized ice during freezing (left side). However, when putting the Petri dish in an open system, steam water condensed from the air would become frozen on the surface of the CB and CGC, which can be removed by hand, and showed amorphous solid of the CGC (right side). (E) Similarly, the CGC was in an amorphous solid phase during cryotherapy in liquid nitrogen after being applied on the cartilage surface. (F) The TGA curve of the hyaline cartilage after treating porcine distal femur with different formulas of cryoprotectants (CB solution for 24 hours, CGC for 24 hours, 60 minutes, and 15 minutes, $n = 4$) also showed significant change in water contents when compared with the control group, indicating permeation of the CGC can be achieved within 15-60 minutes. CGC = cryoprotectant-gel composite; LN = liquid nitrogen; PBS = phosphate-buffered saline; CB = cryoprotectant base; TGA = thermogravimetric analysis.

minutes of slow thawing. The specimens would be then soaked in phosphate-buffered saline (PBS) for another 15 minutes.⁶ For specimens pretreated with either CB or CGC, the cryoprotectants were applied on the articular cartilage surface for 5 minutes in the rat model and for 15 minutes in the porcine model in room temperature, followed by direct LN soaking and freezing. The cryoprotectants would be removed when being soaked in PBS for 15 minutes after the slow thawing phase. All specimens were then placed in PBS for 24 hours before further analysis (**Fig. 1A-C**).

We performed cartilage roughness analysis, loss of proteoglycan, and TUNEL (terminal deoxynucleotidyl transferase dUTP nick end labeling) assay of superficial chondrocytes and subchondral bone for the rat model. Finally, we used Western blot analysis of the cartilage layer among the different groups. For the porcine model, we measured macroscopic clefting of the joint surface, and analyzed decrease of cartilage luminance to examine water loss after cryoinjury and histological and metabolite analysis methods to understand the viability of chondrocytes after freezing among 4 groups.

Quantifying Roughing of Cartilage Surface after Freezing in the Rat Model

After freezing, all rat samples were subjected to analysis after hematoxylin and eosin (H&E) staining to examine articular roughing. Surface roughing was defined as loss of superficial chondrocytes on the articular surface, as seen under 100x microscopic examination. The cartilage roughing surface length compared with the total length of the cartilage surface on each slide was obtained and analyzed ($n = 6$).

Quantifying Matrix Depletion after Freezing in the Rat Model

To evaluate the ability of different cryoprotectants to prevent matrix from depletion during cryotherapy, we quantified the loss of proteoglycan in different groups after freezing. In brief, the cartilage samples ($n = 6$) were sectioned and stained with Safranin-O/Fast Green as measured in the literature.²¹ TIFF image files were captured with a Nikon E600 microscope at 100x magnification and analyzed with ImageJ version 1.5 software (Wayne Rasband, National Institutes of Health, USA). The amount of proteoglycans in different groups was measured according to Afara and Moody's methods^{22,23} and was then compared with the negative control group.

Scoring of Osteoarthritis Change after Cryotherapy on Tissue Slides

To examine the immediate histopathologic changes within the cartilage, 2 senior orthopedic pathologists review slides

and apply the modified Mankin score among different groups.²⁴ The Mankin scoring system assesses superficial structure (0-6), cellularity (0-4), matrix integrity (0-4), and tidemark integrity (0-1). The specimens were examined under 40x microscopy by a senior pathologist ($n = 6$) in each group.

Preparation of the Cartilage Tissue for Western Blot Analysis

To analyze the apoptosis-related protein expression in chondrocytes of the rat model, we extracted cartilage protein using methods modified by Hayashi and his colleagues.¹⁶ Briefly, small fragments of articular disks harvested from the distal femur of rats were washed in PBS (TONYAR Biotech, Taoyuan, Taiwan), and the chondrocyte lysate was collected for Western blot analysis. Immunoblot analysis was performed with the following specific primary antibodies: cleaved caspase-3 (Asp175), cleaved caspase-8 (Asp391), and caspase-9 (C9) (Cell Signaling Technology, Danvers, MA; catalog numbers: 9661, 9496, 9508). Glyceraldehyde 3-phosphate dehydrogenase (GAPDH) (GeneTex, Irvine, CA; catalog number: GTX100118) was used as the loading control. The concentration of primary antibodies was diluted 1:1,000. Chemiluminescence was detected with the UVP BioSpectrum® 600 Image Systems™ (UVP LLC, Upland, CA).

Macroscopic Analysis of Articular Damage after Freezing in the Porcine Model

To evaluate macroscopic articular damage to porcine distal femur after freezing, clefting of the articular surface was counted and compared in different groups ($n = 6$). Briefly, after cryotherapy, the distal femur and articular cartilage were rinsed with Indian ink for 3 minutes; the ink was then washed away with PBS. The cleft of the articular surface of the bilateral femoral condyle would be stained, according to criteria modified from Manil-Varlet and his colleagues.²⁵ The total length of articular clefting was measured and compared.

Analysis of Luminance of Hyaline Cartilage after Freezing in the Porcine Model

After cryotherapy, bilateral condyles of the distal femur were cross-sectioned, and the hyaline cartilage layer was prepared in the same size for analysis ($n = 6$). All specimens were photographed using the same background and camera settings to analyze the luminance of the hyaline cartilage surface after freezing.^{22,26} ImageJ software, version 1.8.0 (Wayne Rasband, NIH, USA), was applied to analyze digital images of articular cartilage. The color tool from the software image menu was open, and Switch Channels was

selected to gain grayscale images of red, green, and blue. The hyaline cartilage specimens were grossly yellow, which provides a strong contrast in the blue channel. We selected 15 different areas of the same size on each specimen to measure the gray value (cd/m^2) of the hyaline cartilage on the histogram, representing the cartilage's luminance level and enabling us to obtain a mean value. The difference in luminance level on the cartilage of different groups was compared and analyzed.

Evaluation of Cryoinjury of Chondrocytes of Cartilage after Freezing in the Porcine Model

The cartilage specimens of the porcine model were also stained with Safranin-O/Fast Green for articular chondrocyte evaluation. The chondrocytes in the superficial to the upper-middle layer of the cartilage are flatter and smaller with a greater density than the deeper layer.⁸ The integrity of superficial chondrocytes is also crucial and imperative in the protection and maintenance of deeper layers.⁸ Therefore, in this part of the study, we would like to observe morphological changes of this layer after a different therapy. Cryoinjury of the superficial chondrocytes was defined as vacuolation or empty lacuna formation of cytoplasm, with concomitant nucleus degeneration, as well as shrinkage of the nucleus, as described previously by Hayashi *et al.*,¹⁶ Muldrew *et al.*,²⁷ and Sotres-Vega *et al.*²⁸ Under 400x microscopy, we calculated degenerated chondrocytes and compared this with all chondrocytes in the superficial layer of the cartilage ($n = 6$). We would also use the TUNEL assay and other immunohistochemical methods (described later) to verify the viability of other parts of the cartilage.

Histological Detection of Apoptotic Cells in Both Rat and Porcine Model

The TUNEL assay on tissue slides to confirm the histological finding in the rat model was performed using *In Situ* Cell Death Detection Kit, POD (Roche, Basel, Switzerland) and modified according to our previous experience.²⁹ In brief, tissue slides were fixed in 4% (wt/vol) paraformaldehyde and permeabilized with 0.3% 0.1% Triton® X-100 solution (BioShop; TRX506). The slides were washed and then incubated with a TUNEL reaction mixture at 37 °C for 1 hour.

Immunohistochemical (IHC) staining was performed on the porcine model to identify caspase-3-dependent apoptotic cells precisely. Super Sensitive™ Polymer HRP Kits IHC (QD420-YIKE; BioGenex, Fremont, CA) was used for analysis. In brief, tissue slides were treated with proteinase K solution at 37 °C for 15 minutes and then blocked by 3% H_2O_2 for another 10 minutes. The slides were incubated

with caspase-3 polyclonal antibody (rabbit anti-porcine 1:1,000; Cell Signaling Technology) overnight at 4 °C and then treated with Super Enhancer for 10 minutes. After being washed with PBS, the sections were immersed in polymer-HRP (horseradish peroxidase) reagent for 30 minutes and can be visualized after adding diaminobenzidine (DAB).

The slides of both rat and porcine models were then examined under a Zeiss AXIO Imager A1 microscope. The quantification of TUNEL-positive apoptotic cells or caspase-3-positive cells was determined by Image J version 1.5 software and performed under microscopic examination in the rat and porcine models ($n = 6$, respectively).

Double Labeling of the Cartilage Tissue with In Situ TUNEL and Caspase-3 IHC Stain on the Porcine Model

To identify live and dead cells on porcine articular cartilage, we used double labeling of TUNEL and caspase-3-positive cells in the middle cartilage layer and area around the tide-mark. In brief, we used *In Situ* Cell Death Detection Kit, POD (Roche) for the TUNEL assay on the slides. After proteinase K treatment, the slides were immersed in the TUNEL reaction mixture (green fluorescence) at 37 °C for 1 hour, after which the sections were incubated with caspase-3 polyclonal antibody (rabbit anti-porcine 1:500; Cell Signaling Technology) overnight at 4 °C for double staining. After washing with PBS, the slides were incubated with a secondary antibody with red fluorescence (1:200, Dylight594 IgG antibody; Genetex) for 1 hour. The nuclei of all cells were counterstained with 4',6-diamidino-2-phenylindole (DAPI; ab104139; Abcam, Waltham, MA), showing blue fluorescence. The slides were then examined under a Zeiss AXIO Imager A1 microscope. Quantification of TUNEL-positive and caspase-3-positive apoptotic cells was determined by Image J version 1.5 software and performed under microscopic examination at both cartilage and subchondral area in the porcine model ($n = 6$).

Cartilage Tissue Viability after Cryotherapy in Porcine Model

The LIVE/DEAD® Viability/Cytotoxicity Kit (Thermo Fisher Scientific Inc., Waltham, MA) was applied to discriminate live from dead cells of the cartilage tissue after cryotherapy. The hyaline cartilage layer was harvested after cryotherapy. We simultaneously stained live and dead cells with green-fluorescent calcein-AM and ethidium homodimer-1 (EthD-1), respectively. Quantification of live and dead cells was performed immediately under microscopic examination. We also cultured cartilage tissue on the Petri dish to verify our results.

Table 1. Primers for Real-Time Quantitative Polymerase Chain Reaction.

Genes	Forward	Reverse	Accession No.	Size
ACAN	GCGGCCACCATCAGAAACCT	CTCCAGGCGTGTGGCAAAGA	NM_001164652	82 bp
COL2A1	TGCCTGGTGTAGAGAGGACGG	GGCCTGGTTGACCGTCGTTG	XM_021092611	72 bp
GLUDI	GCACGGTGGAAACCATTCCCAT	TGTGCGCATGATTTGCCTGG	NM_001244501	133 bp
GAPDH	AAGCATGTGGGGGACTTGGATG	TGGAACCTGCCGTGGGTGGAA	NM_001206359	198 bp
SOX9	CGGCGGAGAAAGTCGGTGAA	GCGTTGGGAGAGATGTGCGT	NM_213843	77 bp

Metabolic Analysis of Articular Cartilage after Cryotherapy in Porcine Model

After cryotherapy, some articular cartilages of different groups were harvested from the porcine femur and briefly rinsed with PBS. Total RNA was isolated using a TriRNA Pure Kit (Geneaid Biotech, New Taipei City, Taiwan), and complementary DNA (cDNA) was synthesized using an iScript™ cDNA Syn-thesis Kit (Bio-Rad, Berkeley, CA) according to the manufacturer's instructions. A real-time quantitative polymerase chain reaction (RT-qPCR) was performed using a StepOne® real-time PCR System (Thermo Fisher Scientific Inc.) with the Smart Quant Green Master Mix with ROX (Protech technology, Taipei, Taiwan), under the following cycling conditions: 95 °C for 10 minutes, followed by 40 cycles at 95 °C for 10 seconds and 60 °C for 30 seconds. The cycle threshold for each gene of interest was normalized against the housekeeping gene (*GAPDH*), and relative gene expression levels were determined using the $2^{-\Delta\Delta C_t}$ method compared with the corresponding untreated group. The primer pairs of genes analyzed are listed in **Table 1**.

Statistical Analysis

All statistical analyses for histological data were performed using GraphPad Prism software (GraphPad Software, San Diego, CA). The Kolmogorov-Smirnov test ensured normal distribution, and Bartlett's method to test homogeneity of variances was performed. For parametric data, we used a 1-way analysis of variance (ANOVA) test with *post hoc* Bonferroni's test for analysis. For nonparametric data, we used the Kruskal-Wallis method and Dunn's post-comparison test for analysis. A *P*-value of the 1-way ANOVA test or Kruskal-Wallis test was considered statistically significant at $P < 0.05$, very significant at $P < 0.01$, and highly significant at $P < 0.001$.

Results

CGC Can Permeate into Porcine Hyaline Cartilage at Different Treatment Time

The TGA curve showed that in the control group, about 48.1% of the total weight of the cartilage tissue was left at

100 °C, indicating that about 51.9% of mobile water becomes evaporated. After treatment with cryoprotectants, residual weight in percentage was 68.0% in CB 24-hour group, 63.9% in CGC 24-hour group, 63.4% in CGC 60-minute group, and 60.6% in CGC 15-minute group. The estimated weight loss of mobile water was, therefore, 32.0% in CB 24-hour group, 36.1% in CGC 24-hour group, 36.6% in CGC 60-minute group, and 39.4% in CGC 15-minute group (**Fig. 1F**). When the temperature reached 150 °C, more water molecules were lost, and finally, they were all released around 240 °C in either group. Our TGA analysis provided evidence of permeation of cryoprotectants into the cartilage tissue and therefore resulted in less water loss (replaced by cryoprotectants) when compared with the control group.

CGC Could Effectively Prevent Cartilage Surface from Roughness in the Rat Model

The mean percentage of cartilage roughness was 18.0% ± 7.6% in the control group and became 69.2% ± 8.4% in the LN freezing group. When we applied different cryoprotectants, cartilage roughness was 55.8% ± 9.3% in the CB group and 25.6% ± 6.1% in the CGC group (**Fig. 2A**). The *P*-value was <0.001 after analysis with 1-way ANOVA test (parametric), and the *post hoc* analysis also showed a significant difference ($P < 0.001$) between control versus LN, control versus CB, LN versus CGC, and CB versus CGC, respectively (**Fig. 2B**).

CGC Could Prevent Proteoglycan from Depletion after Freezing in the Rat Model

When freezing with no sufficient protection, the thickness of the proteoglycan was significantly less in the LN and CB groups (27.7% ± 5.8% and 39.7% ± 6.1% of the control group, respectively). When pretreated with CGC on the joint surface, loss of proteoglycan was significant, with up to 87.5% ± 7.1% of proteoglycan compared with the control group being preserved (**Fig. 2C**). The *P*-value was <0.001 after analysis with the 1-way ANOVA test (parametric), and *post hoc* analysis also showed a significant difference ($P < 0.001$) between control versus LN, control versus CB, LN versus CGC, and CB versus CGC, respectively (**Fig. 2D**).

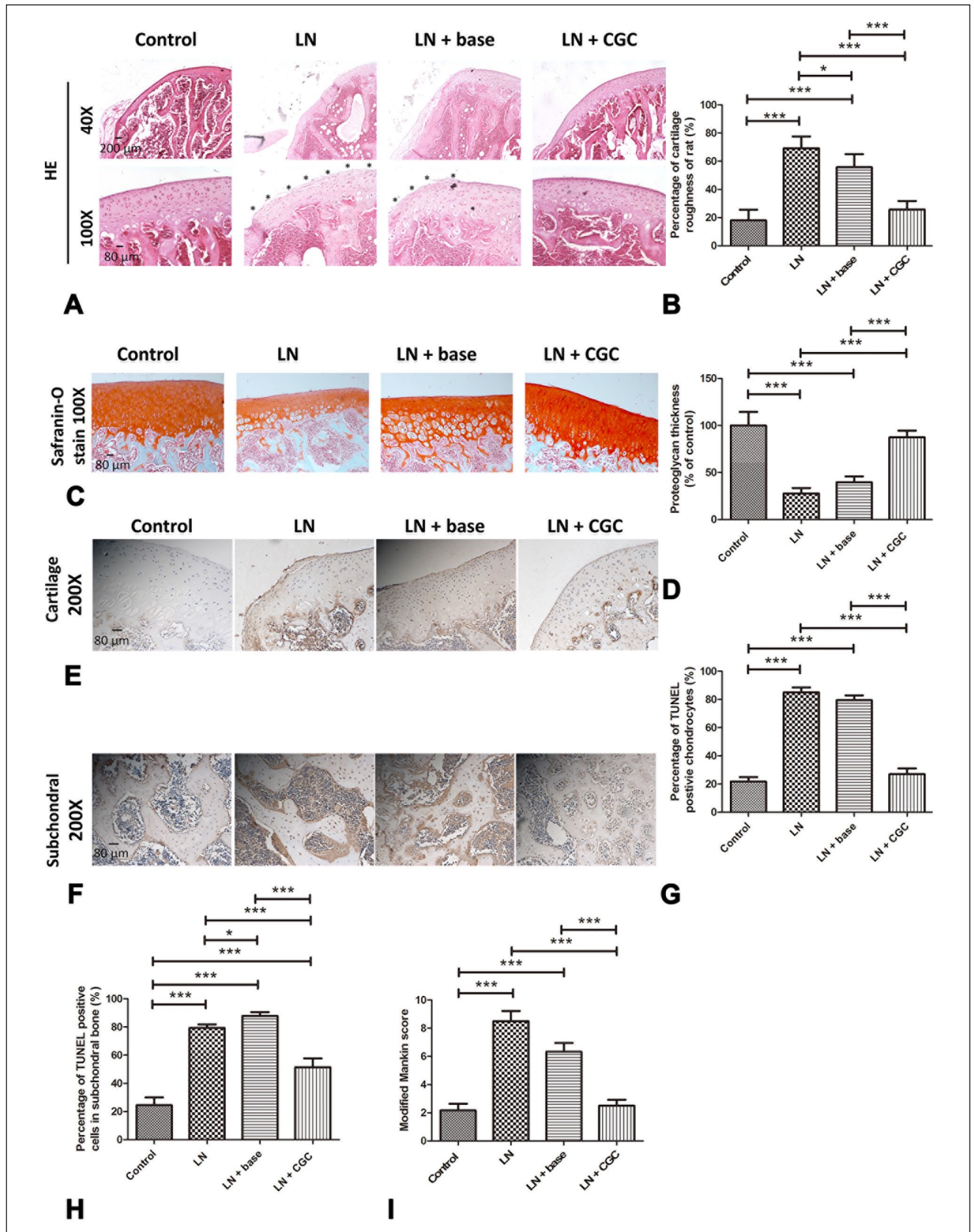


Figure 2. (continued)

Figure 2. Histologic analysis of different cryoprotectants on the cartilage in the rat model. **(A)** H&E stain of cartilage tissue in different groups. After cryotherapy, there was more roughness, increased surface irregularities, and cleaving (*) of the cartilage surface in the LN and LN + base groups. Pyknosis and vacuolated cytoplasm were also observed in the LN and LN + base groups. **(B)** Bar chart analysis of the experiment shown in **(A)**. There was significantly more surface roughness after cryotherapy in the LN and LN + base groups compared with the control and LN + CGC groups. **(C)** Safranin-O stain of the cartilage tissue in different groups. After cryotherapy, a significant reduction of the cartilage matrix proteoglycan was observed in both the LN and LN + base groups. **(D)** Bar chart analysis of the experiment in **(C)**. There was a significant difference in the reduction of the proteoglycan thickness in the LN and LN + base groups compared with the control and LN + CGC groups. **(E)** TUNEL assay of the superficial layer of the cartilage tissue in the rat model. More TUNEL-positive apoptotic cells were observed in LN and LN + base groups than in the LN + CGC group. **(F)** Bar chart analysis of the experiment in **(E)**. The percentage of TUNEL-positive apoptotic chondrocytes was significantly smaller in control and LN + CGC groups compared with the LN or LN + base group. **(G)** In the subchondral area of the cartilage tissue of the rat model, more TUNEL-positive apoptotic cells were observed in the LN, LN + base, and LN + CGC groups compared with the control group. **(H)** Bar chart analysis of the experiment in **(G)**. The percentage of TUNEL-positive apoptotic cells in the subchondral area was significantly higher in the LN, LN + base, and LN + CGC groups compared with the control group. However, when compared with the LN and LN + base groups, significantly fewer TUNEL-positive apoptotic cells were observed in the LN + CGC group, indicating that the protection effect of CGC on cartilage tissue would also extend to some part of the subchondral tissue. **(I)** Histopathologic scoring for early osteoarthritic change in the study groups. The modified Mankin score of the LN + CGC group was significantly lower than that of the LN or LN + base group. LN = liquid nitrogen freezing without protection; CGC = cryoprotectant-gel composite; Control = no treatment; LN + base = pretreatment with cryoprotectant base, followed by LN freezing; LN + CGC = pretreatment with CGC, followed by LN freezing; TUNEL = terminal deoxynucleotidyl transferase dUTP nick end labeling. * $P < 0.05$, ** $P < 0.01$, *** $P < 0.001$.

TUNEL Assay Proved That CGC Could Prevent Mainly Cartilage, Not Subchondral Bone, from Dying during Freezing in the Rat Model

In the cartilage layer, the TUNEL-positive cells were $21.8\% \pm 3.3\%$ in the control group, $85.0\% \pm 3.50\%$ in the LN freezing group, $79.4\% \pm 3.5\%$ in the CB group, and $27.1\% \pm 3.9\%$ in the CGC group (**Fig. 2E**). The P -value was <0.001 after analysis with a 1-way ANOVA test (parametric), and the *post hoc* analysis also showed significant differences ($P < 0.001$) between control versus LN, control versus CB, LN versus CGC, and CB versus CGC, respectively (**Fig. 2F**).

In subchondral bone, the TUNEL-positive cells were $24.6\% \pm 5.5\%$ in the control group, $79.4\% \pm 2.6\%$ in the LN freezing group, $87.9\% \pm 2.7\%$ in the CB group, and $51.5\% \pm 2.6\%$ in the CGC group (**Fig. 2G**). The P -value was <0.001 after analysis with 1-way ANOVA test (parametric), and the *post hoc* analysis also showed significant differences ($P < 0.001$) between control versus LN, control versus CB, LN versus CGC, and CB versus CGC. Though better than LN freezing or CB to prevent subchondral cells from dying, more TUNEL-positive cells in the subchondral bone were observed in the CGC group than in the control group ($P < 0.001$; **Fig. 2H**).

CGC Could Protect the Cartilage from Early Osteoarthritic Change after Cryotherapy in the Rat Model

After treatment, the mean modified Mankin score was 2.2 ± 1.2 in the control group, 8.5 ± 1.8 after LN freezing,

6.3 ± 1.5 in the CB group, and 2.5 ± 1.0 in the CGC group. The P -value was <0.001 after analysis with 1-way ANOVA test (parametric), and *post hoc* analysis also showed significant differences ($P < 0.001$) between control versus LN, control versus CB, LN versus CGC, and CB versus CGC groups, respectively (**Fig. 2I**).

Western Blot Analysis Showed CGC Could Prevent Cartilage from LN-Induced Apoptosis Supported by Caspase-3/8 Apoptotic Signaling Cascade in the Rat Model

Compared with the control group, the cleaved caspase-3 was $190.1\% \pm 11.5\%$ in the LN group, $165.3\% \pm 11.5\%$ in the CB group, and $122.1\% \pm 28.6\%$ in the CGC group (**Fig. 3A and B**). The P -value was 0.002 after analysis with 1-way ANOVA test (parametric), and the *post hoc* analysis also showed significant differences between the control group versus the LN group ($P < 0.01$), the control versus CB group ($P < 0.05$), and the LN versus CGC group ($P < 0.05$).

When trying to pinpoint which apoptotic pathway was involved in frozen-related apoptosis, the expression of the cleaved caspase-8 and cleaved caspase-9 was analyzed in the 4 groups. Compared with the control group, the cleaved caspase-8 was $188.7\% \pm 35.0\%$ in the LN group, $179.7\% \pm 29.5\%$ in the CB group, and $115.0\% \pm 19.8\%$ in the CGC group (**Fig. 3A and C**). The P -value was 0.0055 after analysis with 1-way ANOVA test (parametric) and the *post hoc* analysis also showed significant differences among control versus LN ($P < 0.05$), control versus CB ($P < 0.05$), and LN versus CGC ($P < 0.05$).

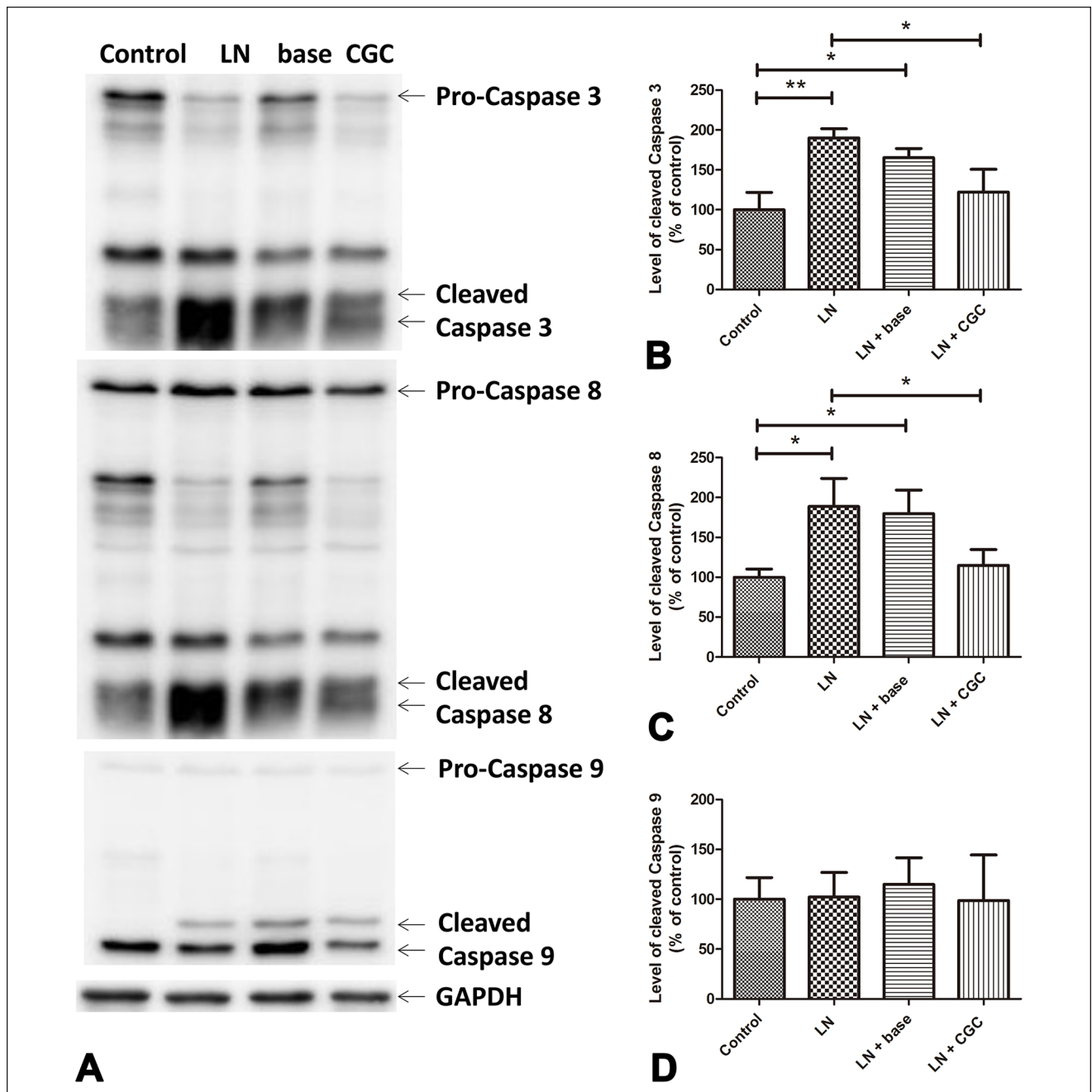


Figure 3. (A) Western blot was applied to analyze the expression of different apoptosis-related proteins (caspase-3, 8, 9) in the cartilage layer of the rat model. (B-C) Bar chart analysis showed significantly higher expression of the cleaved caspase-3 (B) and the cleaved caspase-8 (C) in LN and LN + base groups when compared with the control group. There was no statistical difference in the expression of both cleaved caspase-3 and cleaved caspase-8 in the LN + CGC group when compared with the control group. (D) Bar chart analysis showed no significant differences in the expression of the cleaved caspase-9 among different groups. The above results indicated that CGC could prevent cartilage from LN-induced apoptosis supported by caspase-3/8-dependent extrinsic pathway. LN = liquid nitrogen freezing without protection; CGC = cryoprotectant-gel composite; Control = no treatment; LN + base = pretreatment with cryoprotectant base, followed by LN freezing; LN + CGC = pretreatment with CGC, followed by LN freezing. * $P < 0.05$, ** $P < 0.01$.

Compared with the control group, the cleaved caspase-9 was $102.2\% \pm 24.7\%$ in the LN group, $114.9\% \pm 26.6\%$ in the CB group, and $98.8\% \pm 45.7\%$ in the CGC group

(Fig. 3A and D). The P -value was 0.9133 after analysis with a 1-way ANOVA test (parametric), and the *post hoc* analysis also showed no difference among all groups.

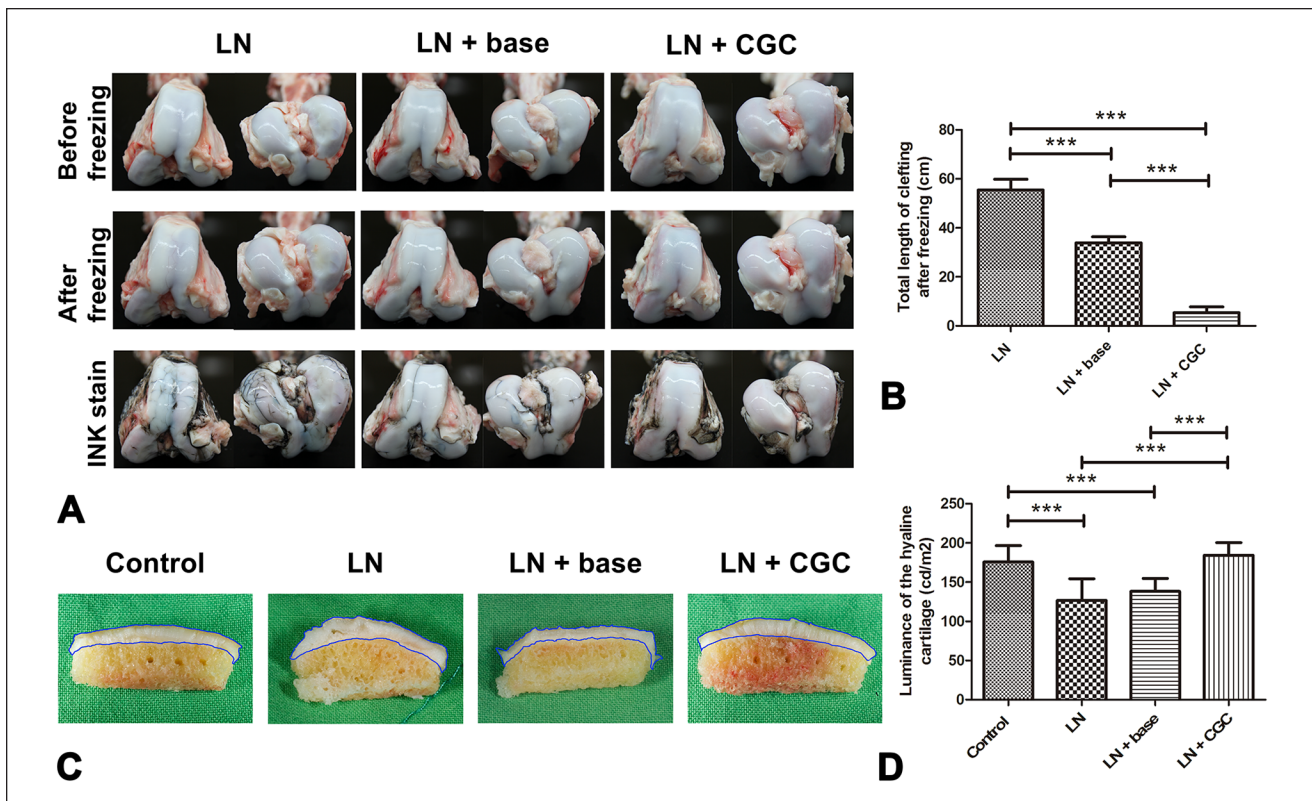


Figure 4. Macroscopic analysis of different cryoprotectants on cartilage protection in the porcine model. **(A)** After cryotherapy, we used Indian ink to stain clefting on the cartilage surface in different groups. Only little clefting was observed in the LN + CGC group when compared with the LN or LN + base group. **(B)** Bar chart analysis of the total length of clefting in different groups showed a significant difference in clefting after cryotherapy. **(C)** Illustration of sectioned femur condyle of porcine distal femur for measurement of luminance by ImageJ software. The blue-circled area represented cartilage tissue subjected to analysis. **(D)** Bar chart analysis of experiment in **(C)**. The mean luminance at hyaline cartilage was significantly higher in control and LN + CGC groups when compared with LN and LN + base groups, which indicates more water loss in frozen, unprotected cartilage if there was no proper vitrification before cryotherapy. LN = liquid nitrogen freezing without protection; CGC = cryoprotectant-gel composite; Control = no treatment; LN + base = pretreatment with cryoprotectant base, followed by LN freezing; LN + CGC = pretreatment with CGC, followed by LN freezing. *** $P < 0.001$.

CGC Prevented Cartilage Surface from Clefting in the Porcine Model

After cryotherapy, the mean of the total length of the surface clefting was 55.42 ± 4.40 cm in the LN freezing group, 33.92 ± 2.48 cm in the CB group, and 5.33 ± 2.42 cm in the CGC group (Fig. 4A). The P -value was <0.001 after analysis with a 1-way ANOVA test (parametric), and *post hoc* analysis also showed significant differences ($P < 0.001$) among the 3 groups (Fig. 4B).

CGC Preserved More Water in the Hyaline Cartilage of the Porcine Model

To evaluate water loss in the porcine model, we measured the luminance of hyaline cartilage before and after cryotherapy among the different groups. The mean luminance at hyaline cartilage was 175.7 ± 20.9 cd/m² in the control

group and 126.8 ± 27.4 cd/m² in the LN group. After applying different cryoprotectants to the articular surface, mean luminance was measured as 138.3 ± 16.4 cd/m² in the CB group and 184.2 ± 16.2 cd/m² in the CGC group (Fig. 4C). The P -value was <0.001 after analysis with a one-way ANOVA test (parametric), and the *post hoc* analysis also showed significant differences ($P < 0.001$) between control versus LN, control versus CB, LN versus CGC, and CB versus CGC groups, respectively (Fig. 4D).

CGC Protected Chondrocytes from Freezing-Induced Degeneration and Caspase-3-Dependent Apoptosis, and Preserved the Integrity of the Cartilage in the Porcine Model

Microscopically, we noted that some clefting in the cartilage layer, as deep as to the tidemark, can be observed in

LN and CB groups after cryotherapy. Moreover, rifting within the matrix of the cartilage can also be observed (**Fig. 5A**). Chondrocyte degeneration (such as vacuolation or empty lacuna with concomitant nucleus degeneration or shrinkage of the nucleus) was $11.4.0\% \pm 4.2\%$ in the control group, $62.9\% \pm 7.4\%$, in the LN group, $51.5\% \pm 5.9\%$ in the CB group, and $20.7\% \pm 5.0\%$ in the CGC group (**Fig. 5A**). The p -value was <0.0001 after analysis with 1-way ANOVA test (parametric), and *post hoc* analysis also showed significant differences between control versus LN ($P < 0.001$), control versus CB ($P < 0.001$), LN versus CGC ($P < 0.001$), and CB versus CGC ($P < 0.001$) (**Fig. 5B**).

IHC stain with caspase-3 antibody of the porcine model showed caspase-3-positive chondrocytes were $18.4\% \pm 4.9\%$ in the control group, $75.2\% \pm 8.7\%$ in the LN group, $60.7\% \pm 9.1\%$ in the CB group, and $31.4\% \pm 6.8\%$ in the CGC group. Moreover, extensive caspase-3-positive apoptotic cells were also noted in the subchondral area of the LN, CB, and CGC groups (**Fig. 5C**). The P -value of caspase-3-positive chondrocytes was $<.001$ after analysis with 1-way ANOVA test (parametric), and the *post hoc* analysis also showed significant differences between control versus LN ($P < 0.001$), control versus CB ($P < 0.001$), control versus CGC ($P < 0.05$), LN versus CGC ($P < 0.001$), and CB versus CGC ($P < 0.001$) (**Fig. 5D**).

The mean of the modified Mankin score was 1.2 ± 0.8 in the control group, 9.7 ± 2.1 after LN freezing, 6.3 ± 2.0 in the CB group, and 2.0 ± 0.6 in the CGC group. The P -value was <0.001 after analysis with 1-way ANOVA test (parametric), and *post hoc* analysis also showed significant differences between control versus LN ($P < 0.001$), control versus CB ($P < 0.001$), LN versus CGC ($P < 0.001$), and CB versus CGC groups ($P < 0.01$), respectively (**Fig. 5E**).

CGC Can Achieve Selective Protection of Articular Cartilage from Freezing-Related Injury in the Porcine Model

We used double labeling of caspase-3 IHC stain and TUNEL assay to discriminate apoptotic cells from necrotic cells in the middle cartilage and the subchondral area. In the cartilage layer, the percentage of TUNEL/caspase-3-positive cells was $69.5\% \pm 8.6\%$ and $58.8\% \pm 12.1\%$ in the LN and CB groups, respectively, whereas the rate was only $2.7\% \pm 1.4\%$ and $5.0\% \pm 2.3\%$ in control and CGC groups. These chondrocytes died mainly through the caspase-3-dependent apoptotic pathway (**Fig. 6A**). The P -value was <0.001 after analysis with 1-way ANOVA test (parametric), and *post hoc* analysis also showed significant differences between control versus LN ($P < 0.001$), control versus CB ($P < 0.001$), LN versus CGC ($P < 0.001$), and CB versus CGC groups ($P < 0.01$), respectively (**Fig. 6B**). Live cells of LIVE/DEAD® assay within the hyaline cartilage were $89.2\% \pm$

5.0% in the control, $3.9\% \pm 1.9\%$ in the LN, $31.9\% \pm 6.1\%$ in the CB, and $65.2\% \pm 8.2\%$ in the CGC groups, respectively (**Fig. 6A**). The P -value was <0.001 after analysis with a 1-way ANOVA test (parametric), and *post hoc* analysis also showed significant differences among all groups (**Fig. 6C**). Chondrocyte culture at day 7 also showed more viable cells in the CGC group (though fewer than the control group) than in the LN and CB groups (**Fig. 6A**).

In the subchondral area, the positive TUNEL and caspase-3 cells were $14\% \pm 3.7\%$ in the control group, $50.5\% \pm 7.7\%$ in the LN group, $39.7\% \pm 5.6\%$ in the CB group, and $26.5\% \pm 4.5\%$ in the CGC group (**Fig. 6D**). The P -value was <0.001 after analysis with 1-way ANOVA test (parametric), and *post hoc* analysis also showed significant differences between control versus LN ($P < 0.001$), control versus CB ($P < 0.001$), control versus CGC ($P < 0.01$), LN versus CGC ($P < 0.001$), and CB versus CGC groups ($P < 0.01$) (**Fig. 6E**). Moreover, when going deeper, more TUNEL(+) caspase-3(-) cells can be observed in the LN, CB, and CGC groups, which has no statistically significant difference among these 3 groups.

Quantitative Real-Time PCR Showed Low Temperature May Still Alter Different Metabolite-Related Gene Expression in the Porcine Model

After cryotherapy, the articular cartilage of different groups was subjected to RT-qPCR for different metabolite analyses (**Fig. 7**). When compared with the control group, the expression of GLUD1 was 0.12 ± 0.06 in the LN group, 0.31 ± 0.08 in the CB group, and 0.82 ± 0.12 in the CGC group (normalized with GAPDH). The P -value was <0.001 after analysis with 1-way ANOVA test (parametric), and *post hoc* analysis also showed significant differences between control versus LN ($P < 0.001$), control versus CB ($P < 0.001$), LN versus CGC ($P < 0.001$), and CB versus CGC groups ($P < 0.001$). The expression of GLUD1 was 0.12 ± 0.06 in the LN group, 0.31 ± 0.08 in the CB group, and 0.82 ± 0.12 in the CGC group (normalized with GAPDH). The P -value was <0.001 after analysis with 1-way ANOVA test (parametric), and *post hoc* analysis also showed significant differences between control versus LN ($P < 0.001$), control versus CB ($P < 0.001$), LN versus CGC ($P < 0.001$), and CB versus CGC groups ($P < 0.001$). The expression of ACAN was 0.15 ± 0.07 in the LN group, 0.12 ± 0.12 in the CB group, and 0.47 ± 0.15 in the CGC group (normalized with GAPDH). The P -value was <0.001 after analysis with 1-way ANOVA test (parametric), and *post hoc* analysis also showed significant differences between control versus LN ($P < 0.001$), control versus CB ($P < 0.001$), control versus CGC ($P < 0.001$), LN versus CGC ($P < 0.01$), and CB versus CGC groups ($P < 0.01$). The expression of COL2A1

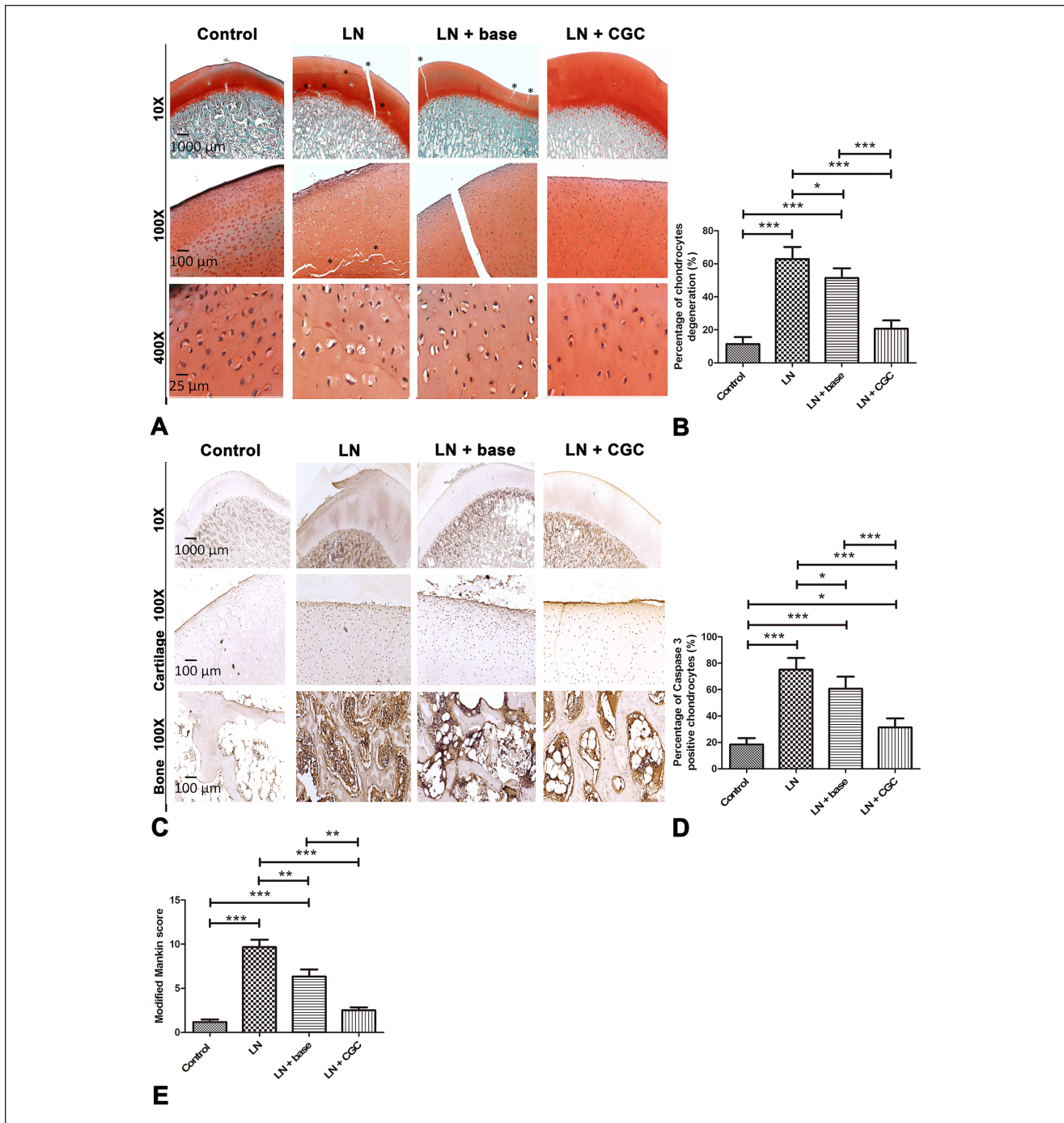


Figure 5. Microscopic analysis of different cryoprotectants on cartilage protection in the porcine model. **(A)** Safranin-O/Fast Green stain of the cartilage tissue in different groups. Microscopically, some clefting on the cartilage (marked with * in 10x images), as deep as to the tidemark, can be observed in the LN and LN + base groups after cryotherapy. Moreover, rifting within the cartilage matrix (marked with * in 100x images) can also be observed in the LN group. Moreover, there were more vacuolated cytoplasm and degenerated chondrocytes as well as hypocellularity in LN and LN + base groups (in 400x images). **(B)** Bar chart analysis among different groups showed significantly more degenerated chondrocytes in LN and LN + base groups. **(C)** IHC stain with caspase-3 antibody of porcine cartilage tissue. More caspase-3-positive apoptotic cells were observed in LN and LN + base groups than in CGC group. **(D)** Bar chart analysis of the experiment in **(C)**. The percentage of TUNEL-positive apoptotic chondrocytes was significantly higher in the LN or LN + base group. **(E)** Histopathologic scoring for early osteoarthritic change in the porcine model. The modified Mankin score of the CGC group was significantly lower than that of the LN or LN + base group. LN = liquid nitrogen freezing without protection; IHC = immunohistochemical; CGC = cryoprotectant-gel composite; Control = no treatment; LN + base = pretreatment with cryoprotectant base, followed by LN freezing; LN + CGC = pretreatment with CGC, followed by LN freezing. ** $P < 0.01$, *** $P < 0.001$.

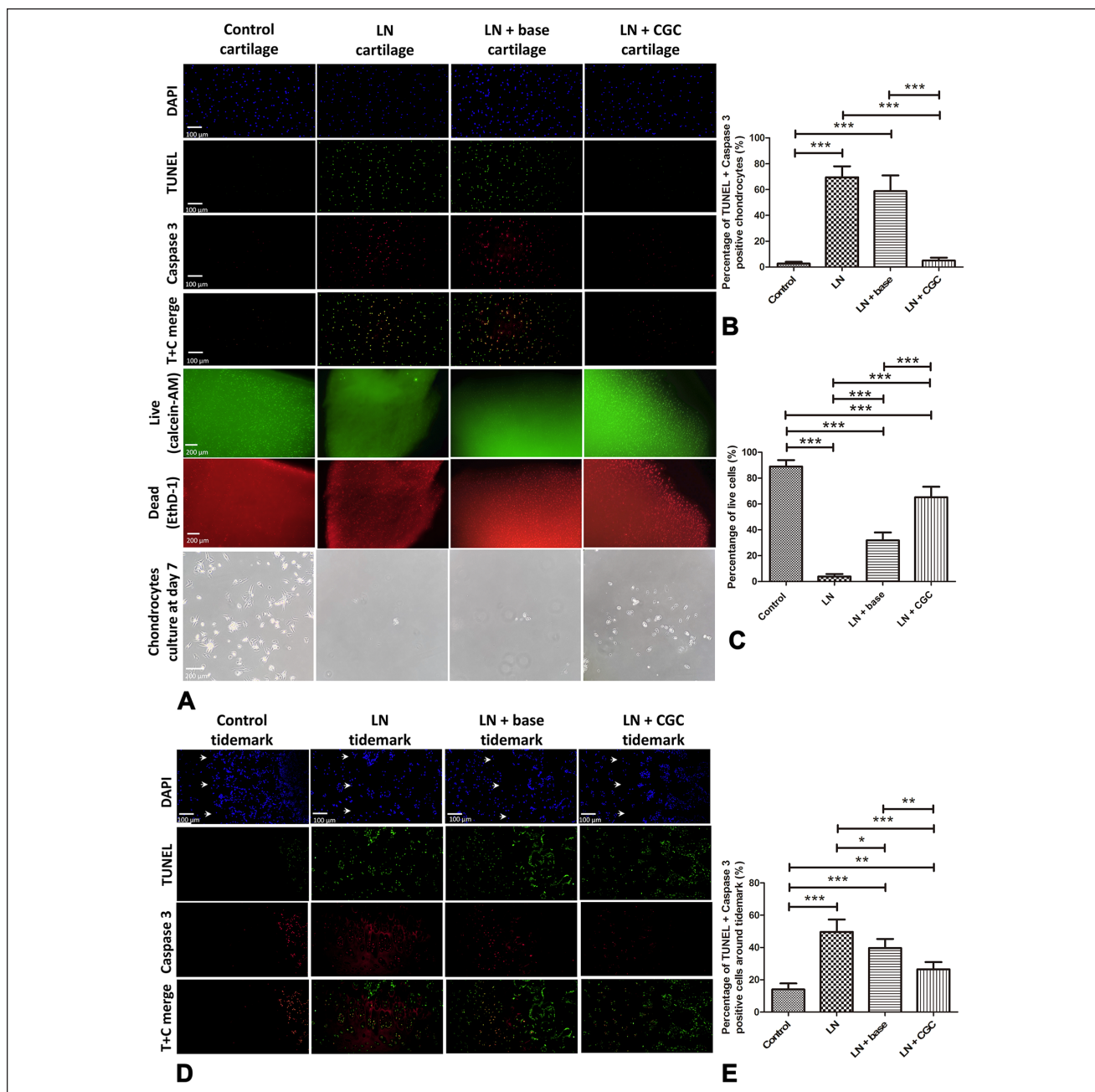


Figure 6. Verification of different methods to protect selectively porcine articular cartilage during freezing. **(A)** In the superficial and middle cartilage layer, double labeling of the cartilage tissue with *in situ* TUNEL and caspase-3 IHC stain showed TUNEL/caspase-3 positive apoptotic cells were more evident in the LN and LN + base groups. LIVE/DEAD® assay of the hyaline cartilage tissue also showed more viable cells in the control and CGC groups. Moreover, chondrocyte culture at day 7 echoed the above finding and showed fewer live cells in the LN and CB groups. **(B)** Bar chart analysis of TUNEL/caspase-3 positive cells in **(A)**. **(C)** Bar chart analysis of live cells on LIVE/DEAD® assay in **(A)**. **(D)** In the subchondral area near the tidemark, TUNEL-and caspase-3-positive apoptosis can be found in the CGC group, but still fewer than the LN and LN + base groups. Moreover, TUNEL (+) caspase-3 (-) necrotic cells can also be found in the LN, LN + base, and LN + CGC groups, indicating that cryoprotectants probably cannot permeate as deep as the bone-cartilage junction. The white arrows indicate the location of the tidemark. **(E)** Bar chart analysis of TUNEL/caspase-3-positive cells in **(D)**. For *in situ* TUNEL and caspase-3 IHC stain: DAPI (blue fluorescence, for all nucleated cells), TUNEL (green fluorescence, for all dead cells), caspase-3 (red fluorescence, for apoptotic cells). For LIVE/DEAD® assay: Calcein-AM (green fluorescence, for all live cells with preserved intracellular esterase activity), EthD-1 (red fluorescence, for all dead cells with loss of plasma membrane integrity). IHC = immunohistochemical; TUNEL = terminal deoxynucleotidyl transferase dUTP nick end labeling; DAPI = 4',6-diamidino-2-phenylindole; LN = liquid nitrogen freezing without protection; LN + base = pretreatment with CB, followed by LN freezing; CGC = cryoprotectant-gel composite; CB = cryoprotectant base; Control = no treatment; LN + CGC = pretreatment with CGC, followed by LN freezing. * $P < 0.05$, ** $P < 0.01$, *** $P < 0.001$.

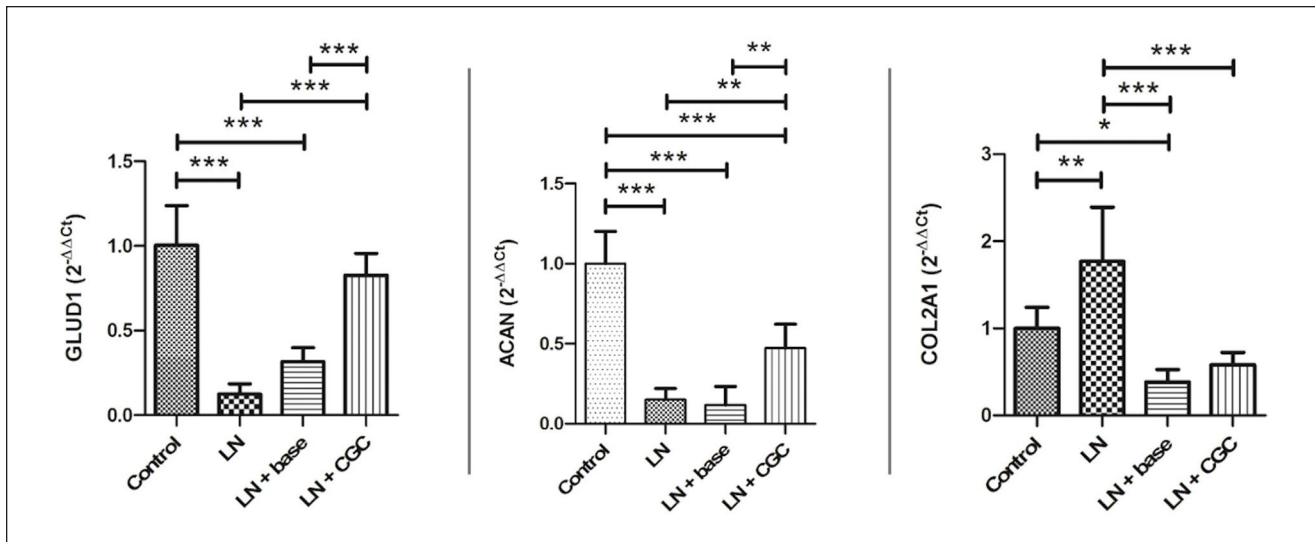


Figure 7. Quantitative real-time polymerase chain reaction of cartilage tissue among different groups, (normalized with GAPDH). Control = no treatment; GAPDH = glyceraldehyde 3-phosphate dehydrogenase; LN = liquid nitrogen freezing without protection; LN + base = pretreatment with cryoprotectant base, followed by LN freezing; LN + CGC = pretreatment with CGC, followed by LN freezing. * $P < 0.05$, ** $P < 0.01$, *** $P < 0.001$.

was 1.77 ± 0.62 in the LN group, 0.38 ± 0.14 in the CB group, and 0.58 ± 0.14 in the CGC group (normalized with GAPDH). The P -value was <0.001 after analysis with 1-way ANOVA test (parametric), and *post hoc* analysis also showed significant differences between control versus LN ($P < 0.01$), control versus CB ($P < 0.05$), LN versus CB ($P < 0.001$), and LN versus CGC groups ($P < 0.001$).

Discussion

The watery environment of hyaline cartilage allows chondrocytes to have a special cellular response in the face of low temperatures. If unprotected, prolonged storage (>14 days) of fresh osteoarticular allografts in the freezer would shift the water within the matrix, reducing the proteoglycan content and causing damage to chondrocytes. The situation would worsen as the temperature falls.^{30,31} Just as vitrification gradually replaced programmed slow-freezing in reproductive medicine, vitrifying articular cartilage has become the mainstream of cartilage preservation.^{10,13,32} If we can successfully vitrify the articular cartilage during tumor surgery, we can perform rapid freezing required to kill tumor cells.^{33,34} So, we tried to design a formula allowing us to apply cryoprotectants on the joint surface alone during tumor surgery.

The selection of cryoprotectants to protect cartilage should have advantages of easy and fast permeation, low toxicity to chondrocytes (which often required a mixture of different cryoprotectants), and faster cooling rate.^{10,11,35,36} We used EG (63%, 10 M) and DMSO (10%, 1.2 M) as our cryoprotectant base to protect cartilage before cryotherapy, for the reason that this formula has the lowest freezing point

among all the formulas we have tried. EG has a very low molecular weight and less toxicity, and is considered a standard part of basic penetrable cryoprotectants.^{13,37,38} Moreover, cells or tissue frozen in EG could also tolerate direct rehydration in the thawing phase, which is more convenient than the traditional step-wise, temperature-controlled method.^{16,17} DMSO is also an effective permeating cryoprotectant, but its toxicity increases, especially at higher concentrations (>6 M) and higher temperatures.^{18,35,39} Combining EG and DMSO can preserve the high permeability rate of cryoprotectants, lower cellular toxicity, and become an acknowledged choice in reproductive medicine.^{13,40} However, our CB was not sticky enough to adhere persistently on the smooth articular surface during surgery. To vitrify cartilage of tumor-bearing bone, we cannot immerse the cartilage, as well as the epiphyseal bone tissue, into the cryoprotectants. Continuously pasting CB on the joint surface is not efficient enough and often results in very limited effects of vitrification. Therefore, we added sodium polyacrylate in 10:1 ratio (CB:sodium polyacrylate) into the CB, which became gel-like CGC. Sodium polyacrylate, also known as water lock, contains sodium, which gives it the ability to absorb large amounts of water. Thus, it becomes a super-absorbent polymer and thickening agent.⁴¹ When mixed with CB, becoming CGC, it could absorb both intracellular and extracellular water exchanged by cryoprotectants. The viscosity would increase at this moment, and the CGC would attach tightly to the articular surface. The CGC is a noncrystalline solid and will not form crystallized ice during freezing, as shown in **Fig. 1D** and **E**. For CGC, the total concentration of cryoprotectants would be around 11.2

M, which is higher than VS55 and other proposed protocols.^{14,15,18,42} According to experiments performed by Jomha and his colleagues, at 22 °C, around 34.6% and 66.8% of EG and around 39.5% and 75.4% of DMSO would permeate into porcine cartilage tissue at 5 minutes and 15 minutes, respectively.³⁵ The predicted permeated concentration of total cryoprotectants after applying CGC for 15 minutes would be more than 6.5 M in our porcine model, which met the concentration required to protect porcine articular cartilage mentioned in previous studies.^{10,11,42} In the rat experiment, because the bone is smaller and the cartilage thinner than in the porcine model, the exposure time was shortened to 5 minutes.

According to the study reported by Unal and Akkus, articular cartilage comprises many forms of water molecules, and free-OH water molecules only account for ~10% of total water in cartilage.⁴³ These loose water molecules are most likely to be replaced by cryoprotectants. Other water molecules will appear in the form of DA-OH (~35%), DDAA-OH (~25%), and DDA-OH (~25%) because of donor-acceptor interaction.⁴³ These networks require higher temperatures to free and evaporate water molecules, especially in a deoxygenated environment, which can be observed in our TGA analysis. After loading different formulas of cryoprotectants on the cartilage, less water loss was noted when compared with the control group, especially in the temperature range of 50 °C-150 °C, indicating certain cryoprotectants might replace some water molecules after exposure. On the other hand, the boiling point of EG and DMSO is around 197 °C and 189 °C, respectively, under regular condition. Therefore, when heating over 200 °C, these cryoprotectants may become vaporized. When the temperature reaches as high as 240 °C, pyrolysis may occur and other organic components within the articular cartilage would be chemically altered and started to char. These processes can explain why the weights of all groups tended to become equalized when reaching 240 °C. In addition, our work also showed that although the effect of cryoprotectant permeation was not as good as soaking whole bone in the CB solution for 24 hours, applying CGC on the cartilage surface for 15 minutes still had satisfying results when compared with the negative control group. Moreover, the TGA results showed that loading CGC for 60 minutes had results comparable to the 24-hour protocols. The degree of reduction in water loss was positively correlated with the time of CGC action. This probably indicates that maybe loading articular cartilage with CGC for longer time (e.g., 30-40 minutes) may be a better alternative for balancing time control, cryoprotectant permeation, and cartilage protection during tumor surgery.

If unprotected, rapid freezing within the articular matrix will result in water depletion and osmotic dehydration.⁹ As the temperature falls, continuous ice formation would create pores within the matrix, disrupting the collagen matrix and

damaging the proteoglycan network.¹⁰⁻¹² The osmotic dehydration would also occur intracellularly. The chondrocytes would become more degenerated with empty lacuna, dense cytoplasm, and irregular nuclei.^{9,14} This can be found more easily in the superficial and middle layer of the chondrocytes because they are elliptical with less cytoplasm in nature. Therefore, degeneration after cryoinjury is more evident and evident than other chondrocytes.¹⁴ In our study, we found more roughness, clefing of the articular surface, and matrix rifting in the LN freezing and CB groups. The clefing and rifting of the matrix can even occur around tidemark. After treatment with CGC, we can observe more preserved integrity of joint surface and cartilage matrix. The degenerated chondrocytes were much fewer, and more elliptical chondrocytes within normally shaped lacuna can also be observed.

After rapid freezing, ice crystals would damage the lipid bilayer of the plasma membrane, membrane-bound nuclei, and organelle, and consequently initiate apoptosis.^{33,34} Hwang and Kim⁴⁴ reviewed studies and indicated that mechanical factors, such as loss of proteoglycan, would induce caspase-3/8-dependent extrinsic pathway and result in chondrocyte apoptosis. In our rat model, we observed many TUNEL-positive dying cells in the cartilage layer of the LN and CB groups after freezing. Moreover, proteoglycan depletion in Safranin-O/Fast Green stain study and Western blot analysis all suggested that the cartilage of the LN and CB groups may undergo caspase-3/8-dependent apoptotic pathway after freezing. In the porcine model, we observed many TUNEL/caspase-3-positive chondrocytes in the cartilage layer of the unprotected cartilage, suggesting that a high concentration of cryoprotectants in the CGC group many protect chondrocytes from dying. In the CB group, because of insufficient cryoprotectant permeation leading to insufficient vitrification, the chondrocytes could not survive after LN freezing. Our LIVE/DEAD® assay proved that CGC, though not as good as the negative control group, could preserve more live chondrocytes than the LN and CB groups, which was also confirmed by our chondrocyte culture results. In the deeper layer near the subchondral area (around tidemark), we observed more apoptotic cells found in the frozen bone of the LN, CB, or CGC group. More necrotic cells were identified in this area in these 3 groups, suggesting that cryoprotectants probably cannot permeate as deep as the bone-cartilage junction. From the above finding, it is possible that CGC selectively protected cartilage, especially the superficial layer, during freezing. Although the effect of vitrification and cryoprotection was not enough in the deeper layer of the articular cartilage, such an effect may just achieve the purpose we developed CGC for tumor surgery: to preserve as much cartilage as we can during LN freezing but not go against our principle of freezing and eliminating tumor cells within the epiphysis and close to the articular cartilage. Future pharmacokinetic studies to determine a more precise

permeation time of CGC in the cartilage matrix are still required to improve our work.

Finally, we used metabolic analysis to understand the function of the chondrocytes among different groups. Glutamine metabolism is critical to control chondrocyte identity and function, and GLUD1 is one of the crucial key enzymes of its metabolism.⁴⁵ Though lower than the control, cartilage tissue of the CGC group had the highest expression of GLUD1 after freezing. Higher expression of GLUD1 in the CGC group indicates it could help cartilage maintain the functions required after cryotherapy. On the other hand, both type 2 collagen and aggrecan are key elements of the proteoglycan network.⁸ Many studies have shown increased expression of both aggrecans and type 2 collagen may occur during late osteoarthritis change.^{46,47} However, compared with aggrecan, which would often increase in the later stage of osteoarthritis, elevated expression of type 2 collagen can be noted in the very early stage of osteoarthritis.⁴⁸ Our results also showed significantly higher expression of type 2 collagen in the LN group. On the other hand, low expression of aggrecan in the LN and CB groups may indicate it was still the early phase of cartilage injury, and the expression level of aggrecan was therefore not yet elevated.

This study had some limitations. In the early stage of developing the CGC, we had tried many different formulas for experimentation. It would be very costly if we used the porcine model for experiments. Therefore, we chose the rat model for testing and then used the porcine model (bone size, cartilage thickness close to human adolescents) for surgical simulation and verification. Second, because we did not use pharmacokinetic model for simulation in the initial stage of the study, we set the vitrification time of CGC by referring to a previous study.³⁵ However, after our TGA analysis and cell viability assay, vitrifying cartilage with CGC for 15 minutes may not be the most appropriate time for vitrification. Although the results of LIVE/DEAD® assay and cell culture showed better results than the LN and CB groups to preserve cartilage cells, it was still not comparable to the negative control group. Applying CGC on the cartilage for 15 minutes seems to provide more structural protection than biological preservation for the cartilage. In the future, we would consider extending vitrifying time of CGC to 30-40 minutes or applying an engineered model set up by Shardt *et al.*¹⁸ to set the best reaction time. Third, we did not transplant the frozen osteoarticular bone graft into the porcine sample to compare the ability of different cryoprotectants to prevent degenerative arthritis after surgery. It requires long-term observation, which is difficult to achieve in existing animal models. Further studies, including animal and pharmacokinetic study on human bone and related metabolic analysis, are required to ensure the safety and efficacy of CGC before applying it in clinical practice.

In conclusion, this animal-based research is the first study to develop a novel cryoprotectant gel aiming to protect cartilage during LN freezing for bony sarcoma. CGC provided

physical protection and prevented articular cartilage from cracking and clefting after LN freezing. It could also provide biologic protection if the appropriate exposure time is determined. Although more works are required to ensure its effectiveness and safety before applying them on the human body, this method may provide a better alternative to preserve native joint for those young children with malignant bone tumor.

Authors' Note

This work was performed in Taipei Veterans General Hospital, Taipei, Taiwan.

Acknowledgments and Funding

The authors wish to thank Dr. Morris Chang and Ms. Sophie Chang for funding our research and manuscript preparation. We would also like to express our gratitude to Pro. Hsin-Lung Chen from National Tsing Hua University for his support in our TGA study. We are also grateful for Mr. Jobs Lin of Daddy Leader Co. Taiwan for their support for our animal study.

Declaration of Conflicting Interests

The author(s) declared the following potential conflicts of interest with respect to the research, authorship, and/or publication of this article: The study has received financial support from Dr. Morris Chang and Mrs. Sophie Chang. The funders had no role in study design, data collection, result analysis, preparation of the manuscript, and had no conflict of interest. All authors certify that he or she has no commercial associations that might pose a conflict of interest in connection with the submitted manuscript.

Ethical Approval

This study is approved by the Institutional Review Board of Taipei Veterans General Hospital, Taipei, Taiwan

ORCID iDs

Chao-Ming Chen  <https://orcid.org/0000-0001-8079-0062>

Yi-Chun Chen  <https://orcid.org/0000-0002-2237-9416>

Po-Kuei Wu  <https://orcid.org/0000-0003-2515-8341>

References

1. Arteau A, Lewis VO, Moon BS, Satcher RL, Bird JE, Lin PP. Tibial growth disturbance following distal femoral resection and expandable endoprosthetic reconstruction. *J Bone Joint Surg Am.* 2015;97:e72.
2. Henderson ER, Pepper AM, Marulanda G, Binitie OT, Cheong D, Letson GD. Outcome of lower-limb preservation with an expandable endoprosthesis after bone tumor resection in children. *J Bone Joint Surg Am.* 2012;94:537-47.
3. Morris CD, Wustrack RL, Levin AS. Limb-salvage options in growing children with malignant bone tumors of the lower extremity: a critical analysis review. *JBJS Rev.* 2017;5:e7.
4. Muscolo DL, Ayerza MA, Aponte-Tinao LA, Ranalletta M. Use of distal femoral osteoarticular allografts in limb salvage surgery. Surgical technique. *J Bone Joint Surg Am.* 2006;88 (Suppl 1, Pt 2):305-21.

5. Hayashi K, Yamamoto N, Takeuchi A, Miwa S, Igarashi K, Higuchi T, *et al.* Clinical course of grafted cartilage in osteoarticular frozen autografts for reconstruction after resection of malignant bone and soft-tissue tumor involving an epiphysis. *J Bone Oncol.* 2020;24:100310.
6. Tsuchiya H, Wan SL, Sakayama K, Yamamoto N, Nishida H, Tomita K. Reconstruction using an autograft containing tumour treated by liquid nitrogen. *J Bone Joint Surg Br.* 2005;87:218-25.
7. Maroudas A, Wachtel E, Grushko G, Katz EP, Weinberg P. The effect of osmotic and mechanical pressures on water partitioning in articular cartilage. *Biochim Biophys Acta.* 1991;1073:285-94.
8. Sophia Fox AJ, Bedi A, Rodeo SA. The basic science of articular cartilage: structure, composition, and function. *Sports Health.* 2009;1:461-8.
9. Ying C, Song FGL, Zhenzhen Chen, Michael J. Taylor, Kelvin G. M. Brockbank. Vitreous preservation of rabbit articular cartilage. *Cell Preserv Technol* 2004;2:8.
10. Abazari A, Jomha NM, Elliott JA, McGann LE. Cryopreservation of articular cartilage. *Cryobiology.* 2013;66:201-9.
11. Jomha NM, Anoop PC, McGann LE. Intramatrix events during cryopreservation of porcine articular cartilage using rapid cooling. *J Orthop Res.* 2004;22:152-7.
12. Zheng S, Xia Y, Bidthanapally A, Badar F, Ilsar I, Duvoisin N. Damages to the extracellular matrix in articular cartilage due to cryopreservation by microscopic magnetic resonance imaging and biochemistry. *Magn Reson Imaging.* 2009;27:648-55.
13. Vajta G, Nagy ZP. Are programmable freezers still needed in the embryo laboratory? Review on vitrification. *Reprod Biomed Online.* 2006;12:779-96.
14. Guan J, Urban JP, Li ZH, Ferguson DJ, Gong CY, Cui ZF. Effects of rapid cooling on articular cartilage. *Cryobiology* 2006;52:430-9.
15. Song YC, An YH, Kang QK, Li C, Boggs JM, Chen Z, *et al.* Vitreous preservation of articular cartilage grafts. *J Invest Surg.* 2004;17:65-70.
16. Hayashi M, Tsuchiya H, Otoi T, Agung B, Yamamoto N, Tomita K. Influence of freezing with liquid nitrogen on whole-knee joint grafts and protection of cartilage from cryoinjury in rabbits. *Cryobiology.* 2009;59:28-35.
17. Onari I, Hayashi M, Ozaki N, Tsuchiya H. Vitreous preservation of articular cartilage from cryoinjury in rabbits. *Cryobiology.* 2012;65:98-103.
18. Shardt N, Chen Z, Yuan SC, Wu K, Laouar L, Jomha NM, *et al.* Using engineering models to shorten cryoprotectant loading time for the vitrification of articular cartilage. *Cryobiology.* 2020;92:180-8.
19. Wang Z, He B, Duan Y, Shen Y, Zhu L, Zhu X, *et al.* Cryopreservation and replantation of amputated rat hind limbs. *Eur J Med Res.* 2014;19:28.
20. Shepherd DE, Seedhom BB. Thickness of human articular cartilage in joints of the lower limb. *Ann Rheum Dis.* 1999;58:27-34.
21. Tran D, Golick M, Rabinovitz H, Rivlin D, Elgart G, Nordlow B. Hematoxylin and safranin O staining of frozen sections. *Dermatol Surg.* 2000;26:197-9.
22. Afara ISS, Moody H, Oloyede A. A comparison of the histochemical and image-derived proteoglycan content of articular cartilage. *Anatom Physiol.* 2013;3:6.
23. Moody HR, Brown CP, Bowden JC, Crawford RW, McElwain DL, Oloyede AO. In vitro degradation of articular cartilage: does trypsin treatment produce consistent results. *J Anat.* 2006;209:259-67.
24. Ma CH, Lv Q, Yu YX, Zhang Y, Kong D, Niu KR, *et al.* Protective effects of tumor necrosis factor-alpha blockade by adalimumab on articular cartilage and subchondral bone in a rat model of osteoarthritis. *Braz J Med Biol Res.* 2015;48:863-70.
25. Mainil-Varlet P, Schiavinato A, Ganster MM. Efficacy evaluation of a new hyaluronan derivative HYADD((R)) 4-G to maintain cartilage integrity in a rabbit model of osteoarthritis. *Cartilage.* 2013;4:28-41.
26. Lahm A, Mrosek E, Spank H, Erggelet C, Kasch R, Esser J, *et al.* Changes in content and synthesis of collagen types and proteoglycans in osteoarthritis of the knee joint and comparison of quantitative analysis with Photoshop-based image analysis. *Arch Orthop Trauma Surg.* 2010;130:557-64.
27. Muldrew K, Hurtig M, Novak K, Schachar N, McGann LE. Localization of freezing injury in articular cartilage. *Cryobiology.* 1994;31:31-8.
28. Sotres-Vega A, Santibanez-Salgado JA, Villalba-Caloca J, Gaxiola-Gaxiola M, Ramos-Abraham C, Rosales-Torres AM, *et al.* Canine tracheal cartilage cryopreservation: freezing injury is not related to caspase-3 expression. *Biopreserv Biobank.* 2013;11:45-50.
29. Wu PK, Wang JY, Chen CF, Chao KY, Chang MC, Chen WM, *et al.* Early passage mesenchymal stem cells display decreased radiosensitivity and increased DNA repair activity. *Stem Cells Transl Med.* 2017;6:1504-14.
30. Pallante AL, Bae WC, Chen AC, Görtz S, Bugbee WD, Sah RL. Chondrocyte viability is higher after prolonged storage at 37 degrees C than at 4 degrees C for osteochondral grafts. *Am J Sports Med.* 2009;37(Suppl 1):24S-32S.
31. Williams SK, Amiel D, Ball ST, Allen RT, Wong VW, Chen AC, *et al.* Prolonged storage effects on the articular cartilage of fresh human osteochondral allografts. *J Bone Joint Surg Am.* 2003;85:2111-20.
32. Csöngé L, Bravo D, Newman-Gage H, Rigley T, Conrad EU, Bakay A, *et al.* Banking of osteochondral allografts, Part II. Preservation of chondrocyte viability during long-term storage. *Cell Tissue Bank.* 2002;3:161-8.
33. Baust JG, Gage AA. The molecular basis of cryosurgery. *BJU Int.* 2005;95:1187-91.
34. Gage AA, Baust JG. Cryosurgery—a review of recent advances and current issues. *Cryo Letters.* 2002;23:69-78.
35. Jomha NM, Law GK, Abazari A, Rekieh K, Elliott JAW, McGann LE. Permeation of several cryoprotectant agents into porcine articular cartilage. *Cryobiology.* 2009;58:110-4.
36. Almansoori KA, Prasad V, Forbes JF, Law GK, McGann LE, Elliott JA, *et al.* Cryoprotective agent toxicity interactions in human articular chondrocytes. *Cryobiology.* 2012;64:185-91.
37. Kasai M. Simple and efficient methods for vitrification of mammalian embryos. *Anim Reprod Sci.* 1996;42:67-75.
38. Jomha NM, Weiss AD, Fraser Forbes J, Law GK, Elliott JA, McGann LE. Cryoprotectant agent toxicity in porcine articular chondrocytes. *Cryobiology.* 2010;61:297-302.

39. Elmoazzen HY, Poovadan A, Law GK, Elliott JA, McGann LE, Jomha NM. Dimethyl sulfoxide toxicity kinetics in intact articular cartilage. *Cell Tissue Bank*. 2007;8:125-33.
40. Li J, Yin M, Wang B, Lin J, Chen Q, Wang N, *et al*. The effect of storage time after vitrification on pregnancy and neonatal outcomes among 24 698 patients following the first embryo transfer cycles. *Hum Reprod*. 2020;35:1675-84.
41. Xu N, Cao J, Liu X. Preparation and properties of water-soluble sodium polyacrylates. *J Macromol Sci Part B*. 2015;54:1153-68.
42. Wu K, Shardt N, Laouar L, Elliott JAW, Jomha NM. Vitrification of particulated articular cartilage via calculated protocols. *NPJ Regen Med*. 2021;6:15.
43. Unal M, Akkus O. Shortwave-infrared Raman spectroscopic classification of water fractions in articular cartilage *ex vivo*. *J Biomed Opt*. 2018;23:1-11.
44. Hwang HS, Kim HA. Chondrocyte apoptosis in the pathogenesis of osteoarthritis. *Int J Mol Sci*. 2015;16:26035-54.
45. Stegen S, Rinaldi G, Loopmans S, Stockmans I, Moermans K, Thienpont B, *et al*. Glutamine metabolism controls chondrocyte identity and function. *Dev Cell*. 2020;53:530-44.e8.
46. Poole AR, Kobayashi M, Yasuda T, Lavery S, Mwale F, Kojima T, *et al*. Type II collagen degradation and its regulation in articular cartilage in osteoarthritis. *Ann Rheum Dis*. 2002;61(Suppl 2):ii78-81.
47. Matyas JR, Ehlers PF, Huang D, Adams ME. The early molecular natural history of experimental osteoarthritis. *Arthritis Rheum*. 1999;42:993-1002.
48. Matyas JR, Huang D, Chung M, Adams ME. Regional quantification of cartilage type II collagen and aggrecan messenger RNA in joints with early experimental osteoarthritis. *Arthritis Rheum*. 2002;46:1536-43.